J Polym Environ (2018) 26:2030–2038
DOI 10.1007/s10924-017-1100-8

ORIGINAL PAPER

Biocompatibility Through Cell Attachment and Cell Proliferation Studies of Nylon 6/Chitosan/Ha Electrospun Mats

Lubna Shahzadi[1] · Rabia Zeeshan[1] · Muhammad Yar[1] · Saad Bin Qasim[2] · Aqif Anwar Chaudhry[1] · Ather Farooq Khan[1] · Nawshad Muhammad[1]

Published online: 23 August 2017

Abstract Novel cefixime loaded chitosan/HA/Nylon 6 electropsun mats were prepared with excellent swelling properties and were tested for cell attachment and cell proliferation. FTIR spectra shows that hydrogen bonding is developed between composite fibers, as pronounced shape change could be seen in amide I and II peaks. SEM analysis displayed completely different morphology (fiber diameters, general appearance, pore-size and shape) of composite fibers as compared to N6 fibers. Composite fibers showed high thermal stability in thermal gravimetric analysis. The ultimate tensile strength of fiber films was around 4.45 MPa. Both composite and Nylon 6 fibers demonstrated sustained drug release up to 24 h. Although the composite and control (Nylon 6) fibers, both, provided compatible favorable environment for the osteoblast cells, the composite fibers provided a better suited environment for the osteoblast cells differentiation and in parallel supporting cellular population also composite fibers exhibited superior swelling properties than the control which in turn complement the healing properties of wound dressings.

Keywords Electrospinning · Chitosan · Nylon · Hydroxyapatite · Composite fibers · Cell proliferation

✉ Ather Farooq Khan
atherfarooq@ciitlahore.edu.pk

✉ Nawshad Muhammad
nawshadmuhammad@ciitlahore.edu.pk

[1] Interdisciplinary Research Centre in Biomedical Materials, COMSATS Institute of Information Technology, Defence Road, Off. Raiwind Road, Lahore 54000, Pakistan

[2] Department of Material Science and Engineering, Kroto Research Centre, University of Sheffield, Sheffield, UK

Introduction

Electrospinning products have increasingly been investigated to be utilized as materials for wound dressings. The electrospun fibers have many useful properties which make them suitable candidate for wound dressing, including high porosity, variable pore-size distribution, high surface to volume ratio, and most importantly, can mimic the extracellular matrix of skin which helps in cell adhesion, migration and proliferation [1, 2]. The advantages of these fibers also comprise of control over evaporative moisture loss of wound, accelerated fluid drainage and inhibition of microbes invasion at wound site [3].

The advance wound dressings also provide the blockade against infection and provide wound harmonious atmosphere, therefore, they have attracted great research exploration [4]. The dressings also provide moist wound environment, minimize the pain and promote wound restoration by rapid epithelialization [5], thus, maximizing the healing rate [6]. Historically, different materials were used as wound dressings such as plant fibers, animal fats and honey pastes [7]. The recent wound dressing reported are mostly composed of hydrogels [8], films [9] and nanofiberous mats [10, 11].

The electrospun fibers can be used for wound dressing applications that may or may not contain wound healing agents [12]. The polymers should be biocompatible and with low/no toxicity. Many polymers are being exploited for electrospun wound dressing for example chitosan (CS), gelatin, poly (lactic acid), polyvinyl alcohol etc. [13]. Composite fibers, derived from biopolymers and synthetic polymers, have biological properties of biopolymers, sufficient spinnability and mechanical strength of synthetic polymers, hence presenting solutions for tissue engineering challenges [14].

Nylon 6 (N6) is a synthetic polymer that bears resemblance to collagen in its backbone and has excellent stability in human body fluid [15, 16]. Additionally, it can easily be electrospun with a wide range of materials [17, 18]. It is being used in medical devices due to its good mechanical properties [19, 20] and has already been proved as an appropriate candidate for bone tissue engineering [21, 22]. However, low-hydrophilicity and biocompatibility hinders its way in biomedical applications. Chitosan (CS) is prepared by alkaline deacetylation of chitin [23, 24] that is one of the most abundant polysaccharide. CS is gradually depolymerized into *N*-acetyl-D-glucosamine which pledges fibroblast proliferation, helps in collagen deposition, maintains improved hyaluronic acid secretion at wound spot thus accelerating wound healing process [1, 24, 25]. Hydroxyapatite (HA) has been used for a number of biomedical implementations like drug release control and bone tissue engineering [26, 27]. Cefixime is a third generation, broad spectrum antibacterial drug especially potent against *Escherichia coli* and *Staphylococcus aureus* bacterial strains that are common cause of wound infections [28, 29]. Previously, researchers have strived to achieve sustained release of cefixime using different polymeric combinations [30].

In this study, the authors have prepared composite N6/CS/HA fibers to overcome the deficits of the respective polymer and ceramic. N6 have imparted good mechanical strength to CS which has poor mechanical strength. On the other hand, the hydrophobicity of N6 is concealed by hydrophilic nature of CS and HA. Afterwards, drug-loading was employed by loading cefixime on both control and composite fibers to observe any difference in release pattern. Further, cell culture and H&E staining was performed to evaluate the behavior of fibroblasts towards the prepared control and composite fibers. The prepared electrospun fibers mats owed to be used in the advance wound dressing materials as well as in tissue engineering and drug delivery can also be exploited.

Materials and Methods

Materials

Nylon 6 (N6, Mw: 10,483) was purchased from Sigma-Aldrich. Chitosan (CS) was synthesized in our laboratories by following the procedure [12] published elsewhere with some modifications [23] (Mw: 146,105 g/mol., degree of deacetylation (DD): 83%, intrinsic viscosity: 30.78 mL/g), hydroxyapatite (HA) sintered powder was purchased from Plasma Biotal Limited (UK). Formic acid (BioM Laboratories Supplies, USA) was of analytical reagent grade and was used without further purification.

Preparation of Control (N6) and Composite (N6/CS/HA) Fibers Mats

N6 (1.2 g) was dissolved in formic acid (10 mL) at 60–70 °C with stirring to prepare 12% (w/v) solution of polymer. The mixture was heated and stirred till complete dissolution of N6. The obtained clear solution was used for electrospinning at 0.2 mL/h injecting rate, 10 cm distance and 20 kV voltages.

For composite fibers, N6 (1.2 g) was dissolved in formic acid (10 mL) at 60–70 °C with stirring to prepare 12% (w/v) solution. To the above solution, chitosan was added (0.096 g, 8% w/w). The mixture was heated gently with stirring to get complete dissolution. Then HA (0.096 g, 8% w/w) was added to the above mixture. The mixture was then used for electrospinning at 0.2 mL/h injecting rate, 10 cm distance and 20 kV voltages.

Morphological Analysis of Fibers

The morphology of the e-spun fibers and films was studied by Scanning Electron Microscope (VEGA3 LMU). The samples were sputter coated with gold, placed on SEM holders and an accelerating voltage of 10 kV was utilized for imaging. Using image-processing software (Image J) the average parameter of 70 pores and the diameters of 100 e-spun fibers were measured from the obtained SEM images. The deeper visible pores on the surface were also considered in the pore's parameter measurement.

Structural Analysis

Chemical structural properties were evaluated by Fourier Transform Infrared Spectroscopy (Thermo Nicolet 6700P, USA). Fourier transform infrared spectroscopy (FTIR) spectra were recorded at room temperature using photo ATR mode with carbon background and nitrogen purging, with resolution of 8 cm^{-1}, 256 scan numbers over the range of 4000–650 cm^{-1}.

Thermal Analysis

Thermogravimetric analysis and Differential Scanning Calorimetry (DSC) was carried out on SDT Q 600(USA) to evaluate the thermal stability and to determine decomposition temperature of N6/CS/HA and N6 e-spun nanofibrous mats. Thermogram was obtained from 25 to 1000 °C at a heating rate of 10 °C min^{-1} under inert nitrogen purge.

Swelling Properties

The swelling ratios of scaffolds were measured as the previous report [31]. Degree of swelling both the control (N6)

and composite e-spun were measured after the samples were submerged in phosphate buffer solution (PBS) at 37 °C for 24 h. Degree of swelling was then measured by using the following formula:

$$\text{Degree of swelling } (\%) = \left[(M - Md)/Md\right] \times 100$$

where M is the weight of each sample after submersion in the buffer solution for 24 h, Md is the weight of the sample after submersion in the buffer solution for specific time interval in its dry state.

Mechanical Testing

The samples were tested for their mechanical strength. Ultimate tensile strength and modulus of elasticity of composite fibers were measured using electrodynamic fatigue testing system series LFV-E 1.5 ME equipped with a load cell of 1.5 kN. The electrospun fiber sheets were 0.03 mm thick with a width of 5 mm and a gauge length of 20 mm was taken for tensile samples. A total of three tensile specimens were tested in order to calculate reliable results. The samples were loaded with cross-head speed of 2 mm/min.

Drug Release Studies

The experiment was designed for evaluating cefixime drug release of electrospun fibers. The method was adopted from a previous study with modifications [32]. Fibers were cut in strips weighing 2–4 mg each along with Nylon 6 strips which were used as control. Cefixime stock solution (1 mg/mL) was prepared in PBS with stirring at room temperature. Each strip was placed in separate sterile vials containing 10 mL of cefixime drug solution. The strips were incubated at room temperature at standing condition for 24 h. After 24 h, the strips were removed and allowed to air dry. Each strip was then weighed after loading.

For release studies, time points were selected 0, 1, 8, 16 and 24 h at room temperature. Each strip was placed (test and control) in separate sterile vials containing 10 mL PBS. At each selected time point, the strips were removed and placed in fresh PBS media. The release media was used to measure cefixime drug release using UV–Vis spectrophotometer at 288 nm.The data was plotted as %age cumulative release as a function of time.

H&E Staining Protocol

MC3T3 cell quantification was done by standard using Haematoxylin&Eosin solutions (H&E) staining protocol. HA/CS/N6 composite and control N6 fibers were seeded with MC3T3 cells for 14 days and retrieved according to the standard protocol. Sample fibers were fixed for 1 h using 3.7% paraformaldehyde (Sigma-Aldrich, USA) in deionized water. This was followed by staining using H&E stains and mounting by DPX mountant (Sigma-Aldrich, USA). The slides were covered by a glass coverslip. Imaging of the slides was done by light microscope (Motic, China).

Cell Studies Protocol

Mouse osteoblast cell line (MC3T3-E1) cells were cultured till they were 90% confluent before seeding. Cell lines were used between passages 3 to 4 in DMEM and seeded in 24-well plates. The transwell containing samples were placed in these culture plate wells in triplicate. MC3T3 were seeded into each well at a population of 20,000 cells per well and allowed to attach for 24 h before placing the transwells. The cell proliferation is determined by Alamar Blue™ assay, which is a colourimetric growth indicator based on detection of metabolic activity. The redox indicator in the solution changes colour from blue to red in response to chemical reduction of Alamar blue into purple by the mitochondrial dehydrogenase activity in cell nuclei. In order to observe cell attachment and viability, fluorescent measurements of Alamar Blue were performed after 1, 4, 7 and 14 days of culturing with MC3T3 cells. For each time point, cell seeded samples were carefully washed with phosphate buffered saline (PBS, Oxoid Tablets, UK) and 0.5 mL of Alamar blue® solution (Sigma-Aldrich, UK) (diluted 1:10 with PBS) is added, followed by incubation at 37 °C for 4 h. Fluorescence was measured at 570 nm using a fluorescence plate reader (Bio-TEK, NorthStar Scientific Ltd, Leeds, UK). Tissue culture plastic (TCP) was used as a control sample and the readings from the samples were subtracted from TCP to obtain the exact absorbance of proliferating cells on specimens. After the measurements, samples were washed with PBS, fresh media was added and the samples were stored in the incubator for the next reading.

Results and Discussion

Morphological Analysis

There are many parameters which affect the morphology and diameter of electrospun fibers. The viscosity and composition of electrospinning solution have significant influence on fiber morphology. Figure 1 displays SAM micrographs of N6 (Fig. 1a) and composite (Fig. 1b) fibers. These e-spun fibers exhibited smooth surface and uniform diameter along their lengths. However, in control fibers (Fig. 1a) the N6 also formed flake like structure. In composite fibers, HA particles were present as a prominent spherical structure. Energy dispersive spectroscopy (EDS) analysis confirmed the CaP nature of these particles. The fiber diameter was found to be in nanometer range. The average diameter of N6

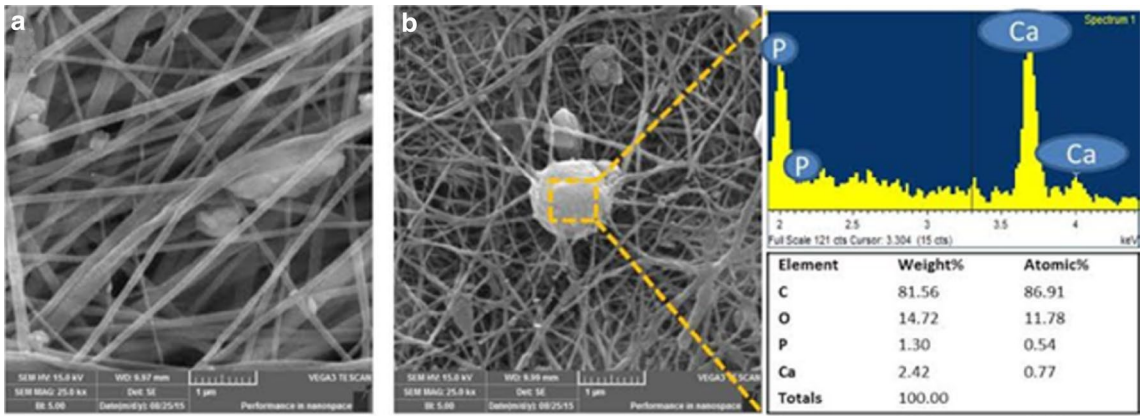

Fig. 1 SEM image of **a** N6 fibers, **b** composite fibers

fibers was 156.96 ± 32.68 nm and that of composite fibers was 60.44 ± 24.87 nm. The average pore diameter of control fibers was 558.76 ± 23.44 nm and that of composite fibers was 240.20 ± 10.84 nm. The decrease in diameter of composite fibers may have resulted due to the change in solution parameters. The parameters that had changed in composite fibers might include viscosity of the solution. It is a well-cited fact that viscosity of electrospinning solution greatly influences the morphology of the fibers. The addition of CS and HA could have changed the solution viscosity which resulted in completely different morphology of composite fibers as compared to control fibers.

The composite fibers displayed completely different morphology than N6 fibers, not only in fiber diameters but also in general appearance, pore-size and shape. It is well-cited fact that pore-size and shape affect cell attachment, proliferation and migration [33]. Also in composite fibers, there were more microfibers present which could provide additional anchor-network for better cell adhesion. EDS analysis of composite fibers also confirmed the incorporation of HA into the electrospun fibers and showed clear peak of Ca.

Structural Analysis

The possible interactions among the used materials were studied by FTIR. The characteristic HA stretching vibration were present at 953, 1008 and 1074 cm^{-1} owing to PO_4.

The stretching vibrations for chitosan O–H and N–H were observed from 3000 and 3550 cm^{-1}. The asymmetrical alkyl peak for C–H stretching was observed at 2881 cm^{-1} and that of symmetrical stretching appeared at 2817 cm^{-1}. Amide I and amide II peaks appeared at 1650 and 1543 cm^{-1}, respectively. The CH_2 bending peaks were present at 1415 and 1381 cm^{-1}. The peak for amide III band was detected at 1322 cm^{-1}. The functional group C–O and ester linkage of chitosan (C–O–C) gave rise the peaks to the peaks at 1117 and 1028 cm^{-1}, respectively. The ring stretching peak of chitosan appeared at 870 cm^{-1}.

In N6 spectra (Fig. 2c), the band at 1632 cm^{-1} is assigned to C=O stretching of the secondary amide band (amide I) as well as the stretching vibrations C=O of polyamide. The amide bands II and III located at 1533 and 1434 cm^{-1}, respectively. Peaks at 1120 and 1074 cm^{-1} were due to the skeletal vibrations involving the C=O stretching. The absorption bands in the 2919 and 2849 cm^{-1} region were characteristic of the stretching vibrations $–CH_2–$ in polyamide backbone. The N6 crystalline α-form peaks at 933, 980, and 1050 cm^{-1} are due to the CONH in-plane vibrations.

The FTIR spectrum of composite fibers (Fig. 2d) confirmed the incorporation of all the components into the fibers. The characteristic peaks of all the components were present in composite fiber spectrum. The N–H stretching peak was observed at 3291 cm^{-1}. The peak was broadened a little and peak intensity decreased. This might be the result of intermolecular hydrogen bonding due to the incorporation of CS and HA in N6. The pronounced shape change could also be seen in amide I and II peaks. These peaks had been split due to formation of hydrogen bonding of C=O group with N–H groups. The ring stretching peaks of CS shifted to 1033 cm^{-1} and N6 α-form peaks at 933 cm^{-1} disappeared in composite fibers. Overall, the spectrum of composite fibers had shown good blend of all the incorporated materials.

Thermal Analysis

The thermal properties of parent and composite fibers were investigated using thermogravimetric analysis (TGA) (Fig. 3). Thermal stability of CS, H6 and composite fibers are shown in TGA thermogram. In N6 fibers, first weight loss was observed around 47 °C which is glass transition temperature (T*g*) of N6 [34]. 10% weight loss was observed in CS and N6 fibers up to 100 °C which might be due to the evaporation of the residual absorbed solvents. The composite

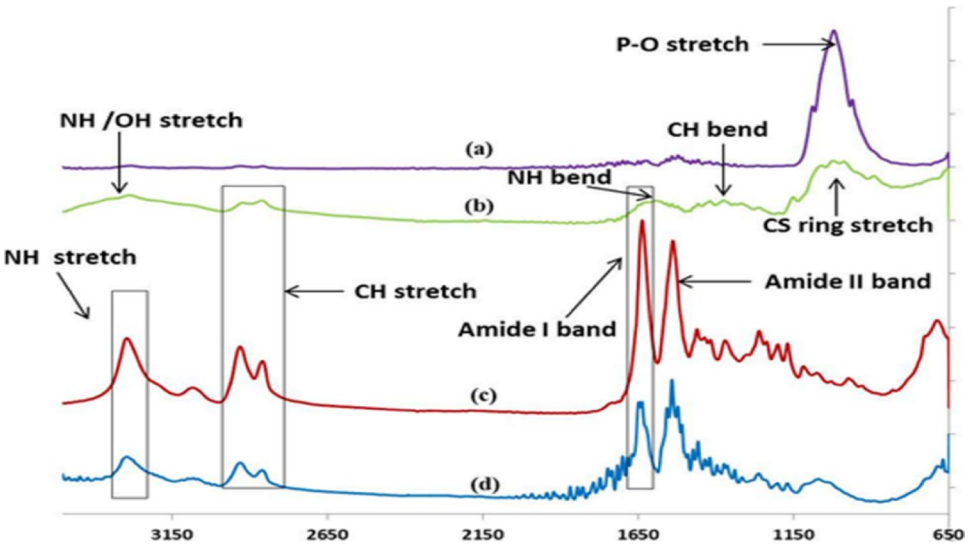

Fig. 2 FTIR results of N6, CS, HA and composite fibers. FTIR spectra in the spectral region (4000–600 cm^{-1}) for (*a*) HA, (*b*) CS, (*c*) N6 fibers, (*d*) composite fibers

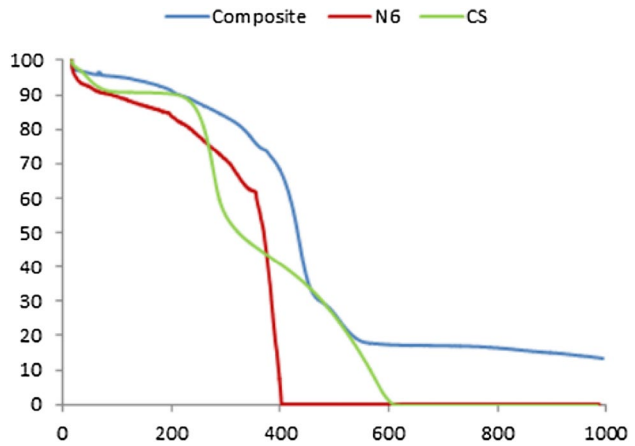

Fig. 3 Thermogravimetric analysis (TGA) of CS, N6 fibers and composite fibers

fibers exhibited more thermal stability and only 5% weight loss was observed over the same temperature range. N6 fiber showed continuous 40% weight loss from 100 to 300 °C which covered the melting point and initial decomposition of polymer. Then there was steep weight loss up to 100% which was due to the complete thermal decomposition of N6 fibers. In case of CS, second sharp weight loss of 45–50% was detected from 220 to 350 °C which was melting temperature range of CS. The third weight loss step in case of CS ranged from 350 to 600 °C which was due to the thermal decomposition of CS and 100% weight loss recorded.

The composite fibers exhibited more thermal stability than the parent polymers; only 10% weight loss was documented up to 220 °C. The reason could be due to the presence of hydrogen bonding among individual components which imparted thermal stability to composite fibers. The statement was well-supported by FTIR peaks of amide and hydroxyl functional groups which clearly indicated the hydrogen bonding among materials through changes in peak shape and intensity. A gradual weight loss of 20% was noted over a temperature range of 250–420 °C. Afterwards a sharp weight loss (40%) was observed over a shorter temperature range of 430–450 °C which could be due to the thermal degradation of polymeric content. Then there was 10–15% weight loss from 450 to 570 °C which is thermal decomposition region of CS. After 580 °C, there was only 2–3% weight loss up to 1000 °C. So, N6 and CS displayed 100% weight loss up to 400 and 620 °C whereas composite fibers exhibited 85% of total weight loss up to 1000 °C which verified their thermal stability as compared to parent polymers.

Swelling Properties

Swelling of composite materials depends on the composition and nature of the polymer used. The e-spun fibers (both control and composite fibers) were soaked in phosphate buffer saline (PBS) solution for 24 h and solution uptake ability was checked after different time intervals i.e. after 1, 4, 8, 16, and 24 h, to check their swelling behaviour. The comparison of solution up-take ability of composite (N6/CS/HA) and control (N6) is shown in Fig. 4. The swelling of N6 fibers was mainly due to the presence of $–NH_2$ and –COOH groups present in the polymer which might have formed hydrogen bonding with solution molecules and also due to the entrapment of solution molecules among electrospun fibers.

The composite fibers displayed excellent swelling properties. Increase in swelling ratio of composite fibers was mainly due to the hydrophilic nature of both CS and HA. $–NH_2$ and –OH functional groups on CS and HA provide hydrogen bonding sites for the solution molecules. Better swelling properties complement the healing properties of

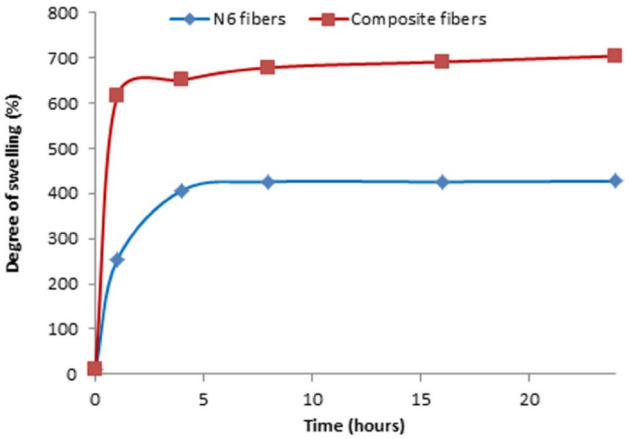

Fig. 4 Percentage swelling of composite fibers and N6 fibers after different time intervals

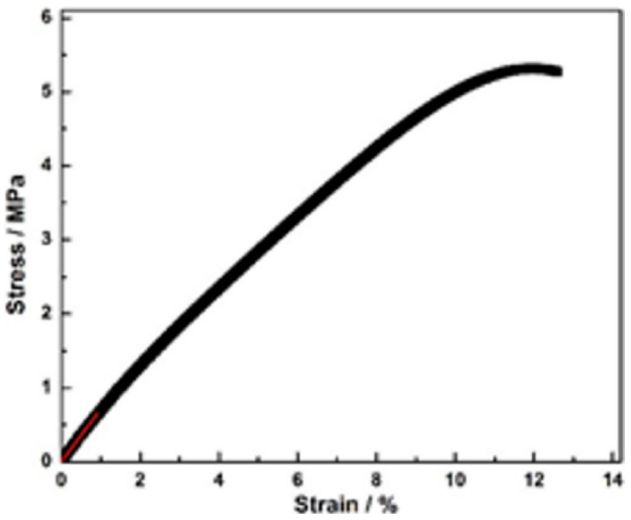

Fig. 5 Stress strain behavior of Nylon 6-Chitosan-HA composite electrospun fiber sheet

wound dressings as it is well-cited in the literature that moist environment accelerates the wound healing process [5, 35]. The composite fibers exhibited two-fold degree of swelling than N6 fibers. It can be seen from Fig. 4 that rapid absorption of solution took place between first 4 h of the experiment. After 4 h, equilibrium was established and there was very little swelling shown by the e-spun fibers.

Mechanical Properties of Composite Fibers Sheet

Mechanical behavior of electrospun fibers sheet was quite consistent which is represented in the stress strain curve shown in Fig. 5. The curve initially showed a linear behavior as represented by red line up to 0.7 MPa and this linear portion was used to calculate modulus of elasticity. On further loading the curve slightly deviated but remained almost linear where it reaches ultimate tensile strength and followed by a stress drop and failure of the sample. The modulus of elasticity calculated from linear region resulted in a value of 62.15 MPa with a standard deviation of 13 MPa. The ultimate tensile strength of fiber films was around 4.45 MPa with a standard deviation of 1.22 MPa. The fiber sheets were failed with at a strain of 13–15%. According to literature [36] chitosan-PVA (30:70) composites showed a similar ultimate tensile strength as determined in this work by making Nylon6-Chitosan-HA (84-8-8%). The electrospun sheet showed slightly low strain to failure due to inclusion of ceramic phase i.e. hydroxyapatite, though their mechanical properties are good enough to be used for dermal applications.

Drug Release Studies

Cefixime is a third-generation antibiotic effectively countering many different bacterial infections. Cefixime loading was carried out by placing the Nylon 6 and composite fibers in 1 mg/mL of drug solution for a period of 24 h. The amount of loaded drug was determined by weighing the fibrous mats before and after drug loading in three separate experiments. The amount of drug loaded was approximately 0.4 mg (13%) for Nylon 6 control fibers whereas a higher loading was seen for the composite fibers corresponding to 0.8 mg (21%) loading. The fibrous structure of the composite facilitated physical adsorption comparably better as compared to the control Nylon 6 fibers. The physical immobilization of cefixime was by simple adsorption or entrapment on the surface and within the matrix which was the case for both control Nylon 6 and composite fibers. Previously, composites of chitosan and HA have shown favorable drug loading and efficient release patterns where the polymer matrix contributes to the controlled drug delivery system [37]. Moreover, surface modifications of these matrices can also be explored and optimized to develop efficient drug entrapment for a controlled drug delivery system.

The aim of this study is to analyze in vitro drug release profile of cefixime-loaded electrospun composite fibers and Nylon 6 fibers as control. The analysis was presented in form of a graph plotted with %age cumulative release versus time (hours). The results obtained for the composite fibers and N6 (control) were comparable (Fig. 6). An initial burst release was observed with in the first hour for both composite and control fibers. 40% of cefixime was released in the initial phased of the drug release study. Previously, it has been reported that due to the presence of drug near or on the surface of the fibers, an initial burst release profile is seen within 10–12 h [38]. In the next 7 h, a small pattern of sustained drug release profile was observed for both the test and control fibers, with 60% of cumulative cefixime drug

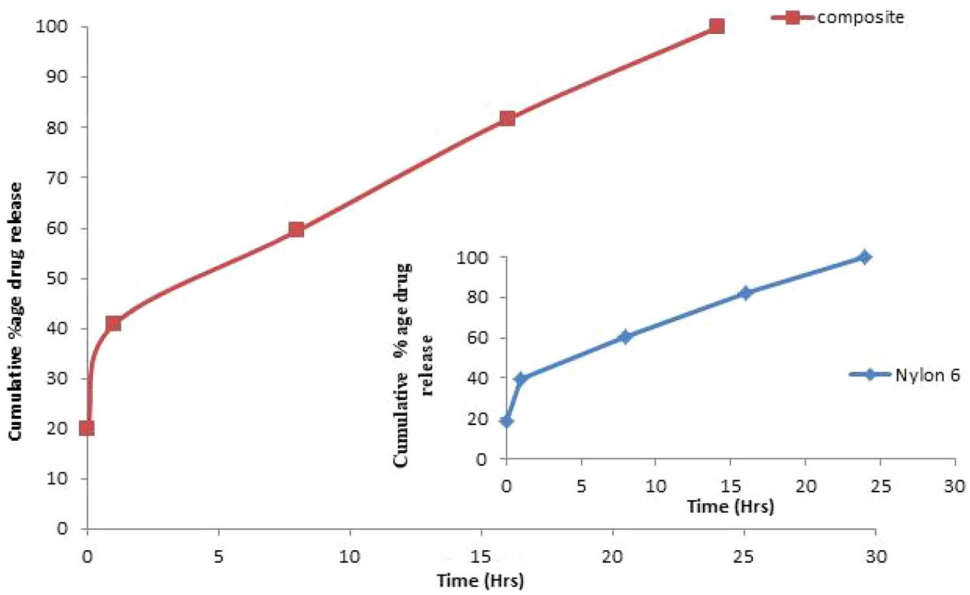

Fig. 6 Cumulative %age drug release from N6 and composite fibers

release. The last phase is marked by a burst drug release profile which was continuous till the 24-hour study for both the composite and control fibers. Cumulative %age cefixime release was seen to increase from 60 to 80% from 8 to 16-h study followed by 100% release profile by 24 h. Decreasing the diameter and fiber distribution can facilitate drug loading within the fibers allowing sustain release of the drug [39]. Previous reports have shown that that if higher amount of drug is loaded in electrospun fibers, it would be present in a crystalline form which results in a burst release implying surface deposition of the drug. Whereas drug loaded inside the fibers is present in amorphous form resulting in a sustain release pattern [40, 41].

Earlier studies have shed light on the advantage provided by the e-spun fibers which can be modulated to deliver drug by versatility subject to the application [39].A drug delivery system's main goal is to achieve targeted delivery governed by accompanying biological cues facilitating site-specific timely dose dependent drug release [42, 43]. The results presented here are indicative that the composite fibers are potential drug delivery system which can cater for a general burst release profile. Owing to a 24-h drug burst release is a promising tool for these composite fibers if to be used in wound dressing. This feature is particularly encouraging since efficient penetration and early treatment of infection is a prerequisite for developing an efficient wound dressing. A delivery system that ensures rapid transport of antibiotics to deal with inflammation either open wounds in case of surgical intervention or a fresh wound, is a vital feature of a wound dressing. Burst release profile as seen, is hence desirable, where the antibiotics play a crucial role within hours to days [44, 45]. Hence supporting these composite fibers are a promising tool for wound dressing owing to their characteristics. Other reports acknowledge the use of Chitosan based delivery system which promoted wound healing and facilitated an initial burst release (24 h) of drug, combating infection [46].

Cell Studies

Metabolic activity and proliferation of osteoblast cells on the composite samples were monitored continuously for 21 days by performing Alamar blue® assay. The absorbance values for the samples were subtracted from the control TCP absorbance values and were represented in the Fig. 7.

In principle, the assay depicts metabolic activity of the osteoblast cells, which is indicative of their proliferative or differentiation stage [47] The potential of CS and HA as components of a system, promoting regeneration by enhancing osteogenesis of mesenchymal stem cells has been reported [48].

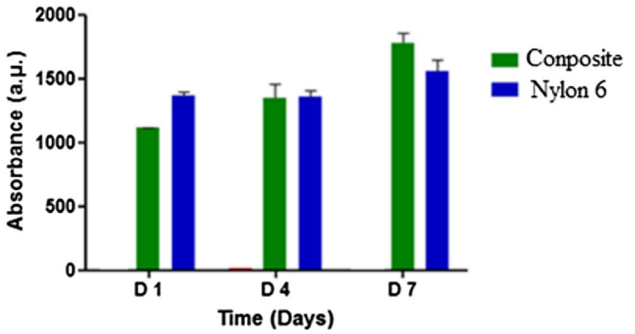

Fig. 7 Cell culture studies of N6 (*blue*) and composite (*green*) fibers. (Color figure online)

Figure 7 represents an overall increase in metabolic activity of the osteoblast cells for N6 and composite fibers over a period of 7 days. Generally, osteoblast cells seeded on N6 fibers represented a higher metabolic activity as compared to the composite fibers. This is suggestive that N6 promotes a consistently high proliferation of the osteoblast cells. Similarly, the same trend was seen on day 4 between the two samples, however, the metabolic activity for the composite fibers were slightly lower than day 1. This decrease in metabolic activity suggests that osteoblast cells shift from proliferation to differentiation. By day 7, the composite fibers sample showed an increase in metabolic activity as compared to day 1, whereas, the control N6 maintained a consistent high metabolic profile throughout the study. Hence, it is evident that the composite fibers facilitated cellular proliferation followed by differentiation which is marked by loss of proliferation. The ability to deliver specific cell types and facilitating their proliferation and sequential differentiation is one feature of a wound dressing, signifying its potential to accelerate the healing process.

H&E Staining

The aim of H&E staining was to evaluate the attachment and proliferation of osteoblast cells on the control (N6) and composite (N6/HA/CS) fibers. Nuclear staining (Fig. 8) confirmed the presence of osteoblast cells.

Cell nuclei were stained blue (Hematoxylin) whereas cells were stained pink (Eosin). Staining analysis indicated that the osteoblast cells were able to nurture consistently along the control Nylon 6 (Fig. 8a–c) and composite (Fig. 8d–f) fibers in a time dependent pattern. This showed that the fibers, as seen in case of both, provided a template that facilitated the growth and attachment of the osteoblast cells. This ability of a material to facilitate cell recruitment followed by proliferation and differentiation holds great promise in regenerative medicine [49]. These composite fibers constituting of biodegradable copolymer can be used to expedite wound healing process for disease conditions. The use of electrospun polymer for skin replacement has been successfully reported [50].

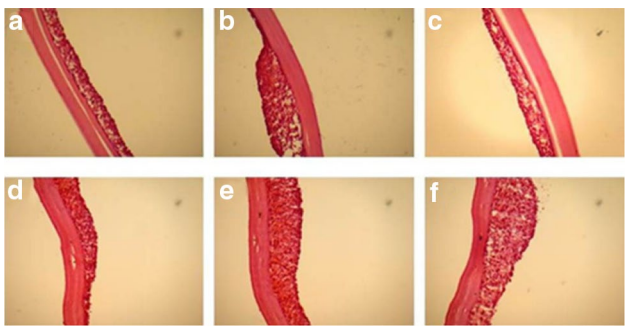

Fig. 8 H&E staining of control (**a–c**) and composite fibers (**d–f**) to evaluate the attachment and proliferation of osteoblast cells

Also in composite fibers (Fig. 8d–f), there is a visible gradual increase in cellular mass and integration of these respective cells with the composite fibers. Osteoblast integration, increase in cellular mass and uniform attachment was more pronounced for composite as compared to control Nylon 6 (Fig. 8a–c) fibers.

Hence, it can be inferred that although the composite and control fibers, both, provided compatible favorable environment for the osteoblast cells, the composite fibers provided a better suited environment for the osteoblast cells differentiation and in parallel supporting cellular population (Fig. 8d–f). The composite electrospun fibers owing to their characteristic three-dimensional structure, promote cellular adhesion and propagate cellular growth and expansion, a feature reiterating their potential application as wound dressing.

Conclusion

In this present research, we have described the successful production of cefixime immobilized Nylon/CS/HA nanofibers. These composite nanofibrous materials delivered drug with excellent swelling properties which make them attractive materials in wound healing applications, adding antibacterial property to its asset. A complete characterization of the synthetized materials was performed including FTIR, SEM and TGA. Smooth fibers were produced after extensive optimization of electrospinning conditions. For drug release studies, a sustained release was observed for 24-h time. Finally, cell culture results showed that these materials were non-toxic and detailed investigations shown that the materials stimulated cells proliferation and also cells were adherent to these materials. We believe these proposed antibacterial wound dressing can serve as the future vanguard for the scientific and industrial community towards future anti-bacterial dressings development.

References

1. Jayakumar R, Prabaharan M, Kumar PS, Nair S, Tamura H (2011) Biotechnol Adv 29(3):322
2. Matsumoto H, Tanioka A (2011) Membranes 1(3):249
3. Schneider X, Wang D, Kaplan J, Garlick, Egles C (2009) Acta Biomater 5(7):2570
4. Song AA, Rane, Christman KL (2012) Acta Biomater 8(1):41
5. Lagana G, Anderson EH (2010) J Nurse Practitioners 6(5):366
6. Pal K, Banthia AK, Majumdar DK (2006) Biomed Mater 1(2):49
7. Majno G (1991) The healing hand: man and wound in the ancient world. Harvard University Press, Cambridge
8. De Cicco F, Reverchon E, Adami R, Auriemma G, Russo P, Calabrese EC, Porta A, Aquino RP, Del P, Gaudio (2014) Carbohydr Polym 101:1216

9. Boateng JS, Pawar HV, Tetteh J (2013) Int J Pharm 441(1):181
10. Shalumon K, Anulekha K, Nair SV, Nair S, Chennazhi K, Jayakumar R (2011) Int J Biol Macromol 49(3):247
11. Unnithan AR, Barakat NA, Pichiah PT, Gnanasekaran G, Nirmala R, Cha Y-S, Jung C-H, El-Newehy M, Kim HY (2012) Carbohydr Polym 90(4):1786
12. Shahzad S, Yar M, Siddiqi SA, Mahmood N, Rauf A, Anwar MS, Afzaal S (2015) J Mater Sci 26(3):1
13. Venugopal J, Ramakrishna S (2010) Appl Biochem Biotechnol 125(3):147 Zahedi P, Rezaeian I, Ranaei-Siadat SO, Jafari SH, Supaphol P Polym Adv Technol 21(2):77
14. Wang C-Y, Zhang K-H, Fan C-Y, Mo X-M, Ruan H-J, Li F-F (2011) Acta Biomater 7(2):634
15. El-Newehy MH, Al-Deyab SS, Kenawy E-R, Abdel-Megeed A (2011) J Nanomater 9:28
16. Pant HR, Bajgai MP, Nam KT, Seo YA, Pandeya DR, Hong ST, Kim HY (2011) J Hazard Mater 185(1):124
17. Abdal-hay HR, Pant, Lim JK (2013) Eur Polym J 49(6):1314
18. Pant HR, Kim HJ, Bhatt LR, Joshi MK, Kim EK, Kim JI, Abdalhay A, Hui K, Kim CS (2013) Appl Surf Sci 285:538
19. Agarwal V, Dougherty R (2001) Google Patents
20. Kiziltas DJ, Gardner Y, Han, Yang H-S (2014) J Polym Environ 22(3):365
21. Pant HR, Baek W-i, Nam K-T, Jeong I-S, Barakat NA, Kim HY (2011) Polymer 52(21):4851
22. Pant HR, Kim CS (2013) Mater Lett 92, 90
23. Farooq A, Yar M, Khan AS, Shahzadi L, Siddiqi SA, Mahmood N, Rauf A, Manzoor F, Chaudhry AA, ur Rehman I (2015) Mater Sci Eng C 56:104
24. Islam S, Bhuiyan MAR., Islam MN (2016) J Polym Environ
25. Paul W, Sharma CP (2004) Trends Biomater Artif Organs 18(1):18
26. Ginebra M-P, Traykova T, Planell J (2006) J Controll Release 113(2):102
27. Zhou H, Lee J (2011) Acta Biomater 7(7), 2769
28. McMillan, Young H, Int J STD AIDS 18(4):253
29. Arshad HM, Mohiuddin OA, Azmi MB (2012) J Appl Pharmaceut Sci 2(1):19
30. Reddy J, Kiran S, Duraival, Pragathi Kumar B (2013) Int J Curr Pharm Rev Res 3:110
31. Liu Y, Ma L, Gao C (2012) Mater Sci Eng C 32(8):2361
32. Shahzad S, Yar M, Siddiqi SA, Mahmood N, Rauf A, Qureshi ZU, Anwar MS, Afzaal S (2015) J Mater Sci Mater Med 26(3):136
33. Lee M, Wu BM, Dunn JC (2008) J Biomed Mater Res A 87(4):1010
34. Khanna YP, Kuhn WP, Sichina WJ (1995) Macromolecules 28(8):2644
35. Field K, Kerstein MD (1994) Am J Surg 167(1):S2
36. Agrawal P (2013) National Institute of Technology, Rourkela
37. Uskokovic V, Desai TA (2014) J Pharm Sci 103(2):567
38. Kenawy el R, Bowlin GL, Mansfield K, Layman J, Simpson DG, Sanders EH, Wnek GE (2002) J Control Release 81(1–2):57
39. Zeng J, Xu X, Chen X, Liang Q, Bian X, Yang L, Jing X (2003) J Control Release 92(3):227
40. Natu MV, de Sousa HC, Gil MH, Int J Pharm 397(1–2):50
41. Zamani M, Morshed M, Varshosaz J, Jannesari M (2010) Eur J Pharm Biopharm 75(2):179
42. Williams GR, Chatterton NP, Nazir T, Yu DG, Zhu LM, Branford-White CJ, Ther Deliv 3(4):515
43. Garcia-Bennett A, Nees M, Fadeel B (2011) Biochem Pharmacol 81(8):976
44. Ko F, Leung V, Hartwell R, Yang H, Ghahary A (2012) Nanofibre based biomaterials—bioactive nanofibres for wound healing applications. In: 2012 International conference on biomedical engineering and biotechnology, pp 389–392
45. Verreck G, Chun I, Rosenblatt J, Peeters J, Dijck AV, Mensch J, Noppe M, Brewster ME (2003) J Control Release 92(3):349
46. Mi FL, Wu YB, Shyu SS, Schoung JY, Huang YB, Tsai YH, Hao JY (2002) J Biomed Mater Res 59(3):438
47. Moore KA, Lemischka IR (2006) Science 311(5769):1880
48. Peng H, Yin Z, Liu H, Chen X, Feng B, Yuan H, Su B, Ouyang H, Zhang Y (2012) Nanotechnology 23(48):485102
49. Shafiq M, Jung Y, Kim SH (2015) J Biomed Mater Res A 103(8):2673
50. Blackwood KA, McKean R, Canton I, Freeman CO, Franklin KL, Cole D, Brook I, Farthing P, Rimmer S, Haycock JW, Ryan AJ, MacNeil S (2008) Biomaterials 29(21):3091